11

Direct Visualization of Single-Molecule DNA-Binding Proteins Along DNA to Understand DNA–Protein Interactions

Hiroaki Yokota
Institute for Integrated Cell-Material Sciences,
Kyoto University
Japan

1. Introduction

Single-molecule fluorescence imaging has recently developed into a powerful method for studying biophysical and biochemical phenomena (Moerner, 2007), including DNA metabolism (Ha, 2004; Hilario & Kowalczykowski, 2010; Zlatanova & van Holde, 2006). While classical biochemical methods yield parameters that are ensemble averaged, single-molecule fluorescence imaging can be used to observe real-time behavior of individual biomolecules, allowing us to study their dynamic characteristics in great detail. Among the various biomolecules, protein molecules, which play central roles in many biological functions, are the prime targets for single-molecule imaging. Direct observations of single-molecule DNA-binding proteins acting on their DNA targets in real time have provided new insights into DNA metabolism. In this chapter, I focus primarily on recent advances in direct visualization of single-molecule DNA-binding proteins *in vitro*, especially on the key techniques employed for this visualization.

2. Fluorophores and fluorescence labeling methods

Direct visualization of protein dynamics by single-molecule fluorescence imaging requires labeling of target protein molecules with a fluorophore. To be used in single-molecule imaging, fluorophores must be (1) bright (have high extinction coefficients and high quantum yield), (2) photostable, and (3) relatively small so as not to perturb the functions of target protein molecules. With regard to photostability, fluorophores in single-molecule imaging tend to undergo photobleaching and blinking (repetitive fluorescence turning-on and -off) because of the high-power excitation. Agents that minimize such photophysical events have been reported (Aitken et al., 2008; Dave et al., 2009; Harada et al., 1990; Rasnik et al., 2006). In general, two classes of fluorophores are used for single-molecule fluorescence imaging: organic small-molecule fluorophores and quantum dots (Qdots) (Table 1). Despite the advantage of the labeling capability with genetic engineering, fluorescent proteins are not popularly applied to single-molecule fluorescence imaging because of their lower intensity and instability of their fluorescence emission. This section briefly describes fluorescence properties of dyes and Qdots and their fluorescence labeling methods.

2.1 Organic small-molecule fluorophores (dyes)

Organic small-molecule fluorophores or dyes with a molecular weight < 1 kDa are mainly used for covalent labeling of protein molecules. Frequently used dyes in single-molecule imaging are Cy3, Cy5, and Alexa derivatives. They emit sufficeint photons to be detected, but subsequently photobleach in approximately 1 minute, and often exhibit blinking (Table 1).

The most popular site-specific labeling method with dyes involves labeling the sulfhydryl group of the cysteine residues with a dye containing a maleimide group. The double bond of the maleimide group may undergo an alkylation reaction with the sulfhydryl group to form a stable thioester bond. The reaction is specific for thiols in the physiological pH range of 6.5–7.5. At pH 7.0, the reaction proceeds 1,000 times faster than its reaction with amines (Hermanson, 2008). Another popular labeling method, which is less site-specific, involves labeling the amine group of amino acids in protein molecules with a dye containing an *N*-hydroxysuccinimide ester (NHS). NHS ester reacts principally with the ε–amines of the lysine side chains and α–amines at the N-terminals (Hermanson, 2008).

2.2 Quantum dots (Qdots)

Qdots are inorganic semiconductor nanocrystals, typically composed of a cadmium selenide (CdSe) core and a zinc sulphide (ZnS) shell measuring 10–20 nm in diameter (Michalet et al., 2005). They are commonly used in single-molecule imaging owing to their resistance to photobleaching and extreme brightness (Table 1). They are characterized by broad absorption profiles, high extinction coefficients, and narrow and spectrally tunable emission profiles, depending on their sizes. Although they are resistant to photobleaching, they often exhibit blinking, which seems to be related to charging of the nanocrystal upon excitation (Table 1). However, recently, the problem of blinking was reported to be overcome by the use of a nanocrystalline CdZnSe core capped with a ZnSe semiconductor shell, in which the transition between ZnSe and CdSe is not abrupt, but radially graded (Wang et al., 2009).

Qdots are usually labeled to protein molecules via immunolabeling. The most popular method is based on an avidin-biotin interaction, an antigen-antibody reaction with the highest affinity. In this method, target protein molecules, which are conjugated with a biotin by chemical crosslinking or genetic engineering, can be labeled with avidin-coated Qdots that are commercially available.

2.3 Advances in site-specific labeling methods

Recent advances in tagging technologies based on genetic have engineering enabled site-specific targeting of fluorophores to protein molecules. One approach is to fuse the target protein molecule to a peptide or a protein recognition sequence, which then recruits a fluorophore coated with the proteins that have affinity for the specific peptide or the protein recognition sequence. For labeling of a Qdot used in single-molecule visualization, HA tag (Kad et al., 2010), Flag tag and HA tag (Gorman et al., 2010), and His tag (Dunn et al., 2011) have been used. Enzyme-mediated covalent protein labeling is also used, in which a recognition peptide is fused to the protein of interest and a natural or engineered enzyme ligates the small-molecule probe to the recognition peptide. This approach can confer highly specific and rapid labeling, with the benefit of a small directing peptide sequence. This

approach involved the following pairs: Halo tag and dehalogenase, biotin ligase acceptor peptide and biotin ligase, and SNAP tag and O^6-alkylguanine-DNA alkyltransferase (Fernández-Suárez & Ting, 2008).

Fluorophore	λ_{em} (nm)	M. W. or size	ε ($M^{-1}cm^{-1}$)	Brightness	Resistance to photobleaching	Resistance to blinking
Dye						
Cy3 maleimide	570	791.0 Da	150,000 (550 nm)	++	++	++
Cy5 maleimide	670	817.0 Da	250,000 (649 nm)	++	+	+
Quantum dot						
Qdot655	~655	~15 to 20 nm	2,100,000 (532 nm)	+++	+++	+
Fluorescent protein						
EGFP	507	32.7 kDa	56,000 (484 nm)	+	+	+

Table 1. Size (or molecular weight) and fluorescence properties of commonly used dyes and a Qdot compared to those of a fluorescence protein.

3. Surface-coating methods

Minimization of the background noise arising from non-specific adsorption of the fluorescently labeled protein molecules on glass substrates is essential for their single-molecule fluorescence visualization. The non-specifically adsorbed protein molecules severely interfere with the visualization because the fluorescence associated with these molecules confounds the fluorescence signal from the target protein molecules. Poly (ethylene glycol) (PEG) and lipid are commonly used for reducing the non-specific protein adsorption on the glass substrate.

3.1 Poly (Ethylene Glycol) (PEG)

PEG is a biocompatible polymer that exhibits protein and cell resistance when immobilized onto metal (Prime & Whitesides, 1991), plastic (Ito et al., 2007), and glass surfaces (Cuvelier et al., 2003), which serves many applications especially in biosensors and medical devices. The feature of PEG comes from its high hydrophilicity and appreciable chain flexibility that induce an effective exclusion volume effect (Harris, 1992). To my knowledge, Ha et al. first used PEG coated glass substrates for single-molecule fluorescence imaging (Ha et al., 2002). The key factors affecting the suppression of nonspecific adsorption by PEG are its length and density (Harris, 1992), both of which are trade-offs. An increase in the chain length of PEG to construct a defined tethered chain layer results in a decrease in the density of the PEG chain due to the exclusion volume effect. PEG with a molecular weight of 5,000 appears to find a compromise between the trade-offs to maximize the suppression of non-specific adsorption of protein molecules on a glass surface (Heyes et al., 2004; Malmstena et al., 1998; McNamee et al., 2007; Pasche et

al., 2003; Yang et al., 1999). A general approach to the immobilization of PEG onto a glass surface involves coupling of PEG to amine groups that have been conjugated on the surface by silanization (Figure 1a). Another approach involves coupling of PEG through poly (L-lysine) adsorption on the surface (Figure 1b). The inclusion of a small fraction of biotinylated PEG provides anchor points for tethering DNA (Section 4).

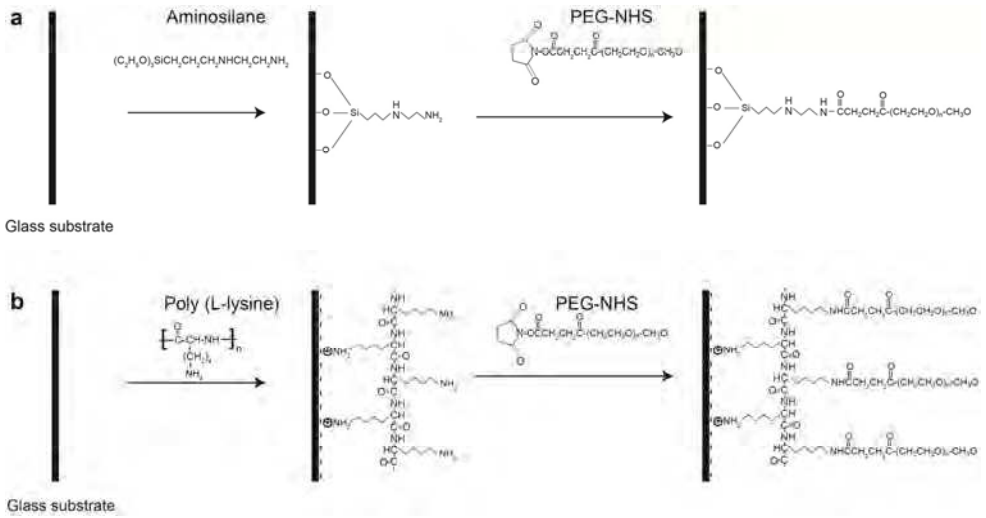

Fig. 1. PEG coating methods of glass substrates through either (a) silanization or (b) poly (L-lysine) adsorption.

3.1.1 PEGylation through aminosilanization

The standard PEG coating method on quartz slides and silicate coverslips for single-molecule fluorescence imaging is performed by silanization with *N*-2-(aminoethyl)-3-aminopropyl-triethoxysilane in methanol containing acetic acid for few hours (Figure 1 (a)) (Joo et al., 2006). The aminosilanization treatment yields a surface that is densely coated with exposed primary amines. A covalently attached PEG layer is formed on the surfaces by a PEGylation reaction with the amine reactive *N*-hydroxy-succinimidyl (NHS)-PEG (M.W. = 5,000 Da) dissolved commonly in freshly prepared 0.1 M sodium bicarbonate buffer (pH 8.3) for a couple of hours.

3.1.2 Improvement of non-specific adsorption suppression capability on silicate coverslips

I found that the standard PEG coating method mentioned above did not suppress non-specific adsorption as effectively on silicate coverslips as it did on quartz (Yokota et al., 2009). Therefore, an improved method for efficient PEG coating on silicates is required to reduce their non-specific adsorption. Then, I found that performing the PEGylation

reaction in 50 mM 3-(*N*-morpholino)propanesulfonic acid (MOPS, pH 7.5) instead of the usual 0.1 M sodium bicarbonate (pH 8.3) reduced non-specific adsorption on silicate surfaces by up to an order of magnitude. Figure 2 shows the single-molecule fluorescence images of a cyanine dye-labeled protein (the *E. coli* helicase UvrD (Lohman et al., 2008) labeled with Cy5: Cy5-UvrD) non-specifically adsorbed on a silicate coverslip that was PEGylated in MOPS buffer as compared to one with no treatment and one coated following the standard method. The improvement is crucial since silicate coverslips are extensively used for single-molecule fluorescence microscopy with epi-illumination (Funatsu et al., 1995), highly inclined thin illumination (Tokunaga et al., 2008), and total-internal reflection fluorescence (Tokunaga et al., 1997) microscopies (sometimes combined with other techniques such as optical tweezers (Hohng et al., 2007; Lang et al., 2004; Zhou et al., 2011)). The improvement in non-specific adsorption using the new buffer condition for PEGylation was also observed on quartz, though to a lesser extent (Table 2) and with a Qdot-labeled protein molecule (UvrD labeled with Qdot655:Qdot655-UvrD) (Table 3). Figure 3 shows the single-molecule fluorescence images of a Qdot-labeled protein (Qdot-UvrD) non-specifically adsorbed on a silicate coverslip that was PEGylated in MOPS buffer as compared to one with no treatment. While PEGylation is required to reduce the non-specific adsorption of Qdot-labeled protein on both silicate and quartz surfaces, PEGylation in MOPS buffer reduced non-specific adsorption of Qdot-UvrD on glass substrates by a factor of approximately 2 as compared to PEG coating in sodium bicarbonate buffer (Table 3). The key issue determining the non-adsorption properties of PEG-coated glass surfaces is their coverage by the polymer (Harris, 1992), which is improved with the new method. PEG coating at pH 7.5 may be enhanced with respect to coating at higher pH owing to better stability of the NHS ester. Its lifetime is in the order of hours at physiological pH and decreases steeply at higher pH owing to increased hydrolysis (Hermanson, 2008).

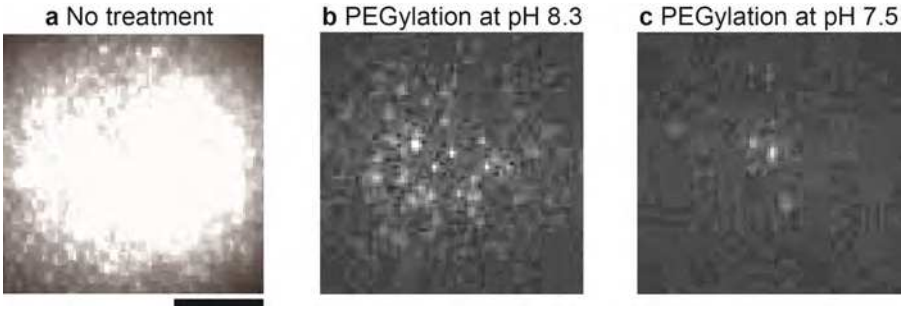

Fig. 2. Enhancement of protein-non-adsorption capability on silicate coated with PEG dissolved in 50 mM MOPS (pH 7.5). Fluorescence images of Cy5-UvrD non-specifically adsorbed on silicate with (a) no treatment, coated PEG dissolved in (b) 0.1 M sodium bicarbonate (pH 8.3) and (c) 50 mM MOPS (pH 7.5). The Cy5-UvrD concentration used was 2 nM. Scale bar, 10 μm.

	Silicate			Quartz		
	No treatment	PEG (pH 8.3)	PEG (pH 7.5)	No treatment	PEG (pH 8.3)	PEG (pH 7.5)
Mean number of Cy5-UvrD non-specifically adsorbed (/nM/1,000μm^2)	1.6×10^3 ±0.5×10^3 (21)	39 ±4 (9)	3.9 ±1.4 (30)	2.2×10^3 ±0.3×10^3 (6)	1.4 ±0.2 (9)	0.78 ±0.20 (13)
Ratio to the number for PEG (pH 7.5)	4.1×10^2	10	1	2.8×10^3	1.8	1

The mean numbers of Cy5-UvrD non-specifically adsorbed per 1,000 μm^2 are normalized by the UvrD concentrations (nM) used for the experiments. Values represent mean ± standard deviation (*n*). (Reproduced from (Yokota et al., 2009) , Copyright (2009), with permission from The Chemical Society of Japan).

Table 2. Protein-non-adsorption capability on silicate coverslips and quartz slides (Cy5-UvrD).

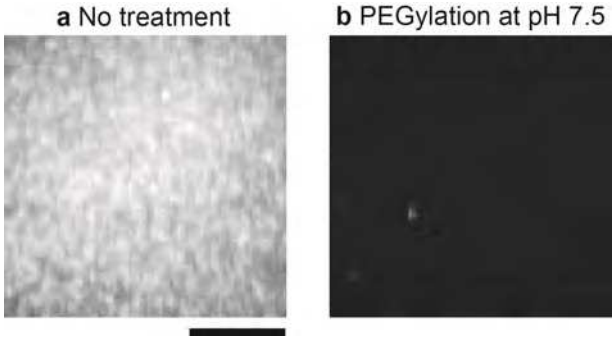

Fig. 3. Reduction of the non-specific adsorption of Qdot-labeled protein on glass substrates coated with PEG dissolved in 50 mM MOPS (pH 7.5). (b) Fluorescence images of Qdot-UvrD non-specifically adsorbed on silicate with no treatmemt (a) and coated with PEG dissolved in 50 mM MOPS (pH 7.5) (b). The Qdot-UvrD concentration used was 1 nM. Scale bar, 10 μm.

	Silicate			Quartz		
	No treatment	PEG (pH 8.3)	PEG (pH 7.5)	No treatment	PEG (pH 8.3)	PEG (pH 7.5)
Mean number of Qdot-UvrD non-specifically adsorbed (/nM/1,000 μm^2)	6.8×10^3 ±0.5×10^3 (8)	1.9 ±0.8 (23)	1.3 ±0.3 (22)	1.6×10^4 ±0.3×10^4 (9)	1.7 ±0.2 (9)	0.51 ±0.20 (9)
Ratio to the number for PEG (pH 7.5)	5.2×10^3	1.5	1	3.1×10^4	3.3	1

The mean numbers of Qdot-UvrD non-specifically adsorbed per 1,000 μm^2 are normalized by the UvrD concentrations (nM) used for the experiments. Values represent mean ± standard deviation (*n*). (Reproduced from (Yokota et al., 2009) , Copyright (2009), with permission from The Chemical Society of Japan).

Table 3. Protein-non-adsorption capability on silicate coverslips and quartz slides (Qdot-UvrD).

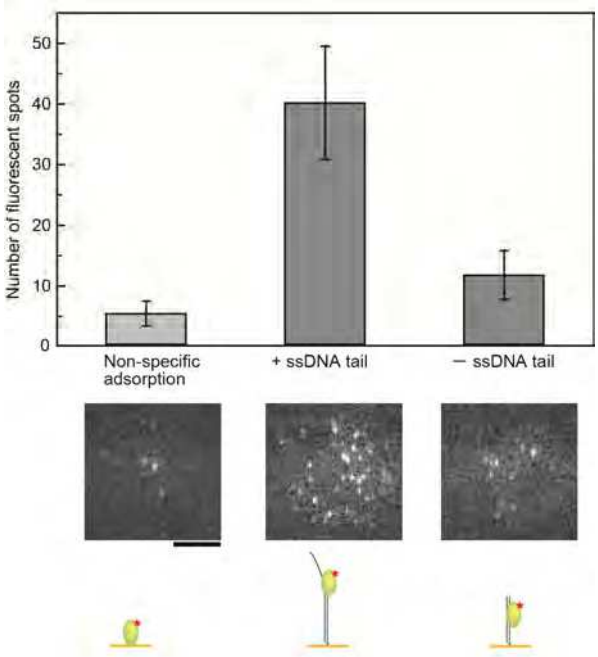

Fig. 4. Comparison of the numbers of Cy5-UvrD interacting with 18-bp dsDNA with or without an ssDNA tail immobilized on a PEG-coated silicate coverslip. Below are the single-molecule fluorescence images. The Cy5-UvrD concentration used was 2 nM. Scale bar, 10 μm. (Reproduced from (Yokota et al., 2009), Copyright (2009), with permission from The Chemical Society of Japan).

The results on the reduction of non-specific protein adsorption on glass surfaces indicate that our PEGylation method facilitates direct visualization of single-molecule interactions between fluorescently labeled protein molecules and DNA. Indeed, we could visualize how Cy5-UvrD interacts with a 18-bp dsDNA with or without an ssDNA tail immobilized on PEG-coated surfaces. The number of Cy5-UvrD fluorescent spots observed can be compared in Figure 4; this figure clearly shows that non-specific adsorption of Cy5-UvrD on the surface was effectively suppressed enough to conclude that Cy5-UvrD has higher affinity for the dsDNA with an ssDNA tail than for that without one; this finding is in agreement with that of a previous report (Maluf et al., 2003).

3.1.3 Single-molecule visualization of binding mode of helicase to DNA on silicate coverslips

Using microscopy, we could compare the number of UvrD molecules bound to 18-nt ssDNA, 4.7-kbp dsDNA, and 4.7-knt ssDNA immobilized on a PEG-coated silicate coverslip. Figure 5 shows a comparison of fluorescence intensity distributions of Cy5-UvrD bound to 18-nt ssDNA, 4.7-kbp dsDNA, or 4.7-knt ssDNA. In agreement with the results in Figure 4, Cy5-UvrD had low affinity for dsDNA, and thus, the fluorescence intensity distribution for 4.7-kbp dsDNA peaked at a fluorescence intensity that corresponds to that

of single Cy5-UvrD, which was validated by the observation that most of the fluorescent spots photobleached in a single step. This was also the case with the experiment using 18-nt ssDNA. For the experiment using 4.7-knt ssDNA, the fluorescence intensity distribution shifted to a larger value, indicating that multiple Cy5-UvrD attached to the ssDNA.

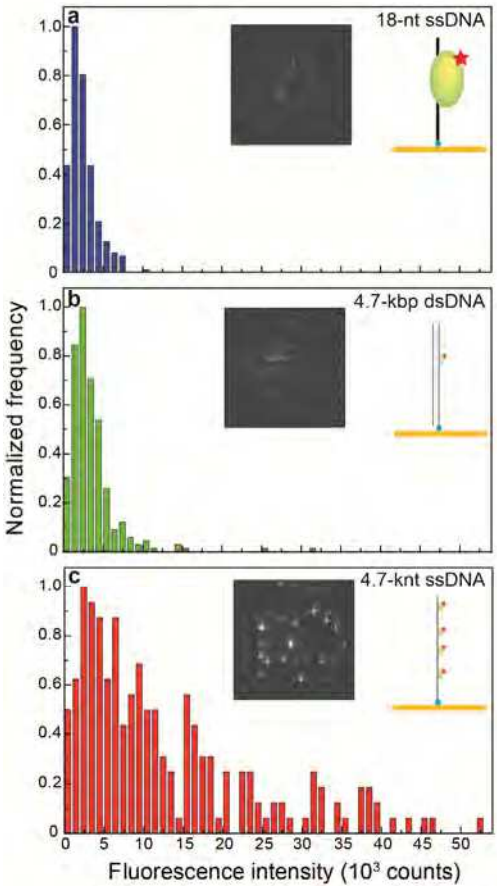

Fig. 5. Comparison of fluorescence intensity distributions of Cy5-UvrD bound to (a) 18-nt ssDNA, (b) 4.7-kbp dsDNA, or (c) 4.7-knt ssDNA immobilized on a PEG-coated silicate coverslip. The insets show the single-molecule fluorescence images. The Cy5-UvrD concentration used was 2 nM. Scale bar, 10 μm. (Reproduced from (Yokota et al., 2009) , Copyright (2009), with permission from The Chemical Society of Japan).

3.1.4 Stability of PEG-coated surfaces

The long-term stability of PEG has been examined in several studies. On examination of a PEG-coated coverslip surface for up to 1 month, the surface, immersed in 0.1 M sodium phosphate buffer (pH 7.4), has been found to degrade after 25 days (Branch et al., 2001). Another study examined the stability of PEG-modified silicon substrates that were

incubated in PBS (37 °C, pH 7.4, 5% CO_2) for different periods of time up to 28 days. This study also concluded that PEG-modified surfaces retain their protein and cell repulsive nature for the period of investigation, i.e., 28 days (Sharma et al., 2004). With regard to PEG stability in the air, no degradation was reported after 75 days (Anderson et al., 2008). In contrast to these macroscopic experimental studies, PEG-coated surfaces used for single-molecule imaging imposes several challenges. The protein-non-adsorption capability of PEG-coated glass surfaces sharply deteriorated with time (incubation > 24 h) when incubated in a buffer (Yokota et al., 2009). Moreover, PEG-coated coverslips and quartz slides exhibited increasing non-specific adsorption with time when stored, exposed to the air, at room temperature (Yokota et al., 2009). PEG is known to degrade by oxidation (Han et al., 1997), and thus, to prevent the oxidative degradation, PEG-coated slides/coverslips can be stored in the dark under dry conditions at –20 °C until use (Joo et al., 2006).

3.1.5 PEGylation through poly(L-lysine) adsorption

PEGylation is also feasible through poly(L-lysine) adsorption on the glass surface (Figure 1b). The amino groups of the side chain of poly(L-lysine) are positively charged at pH values below 10, and are therefore easily attached to the negatively charged glass surface (Iler, 1979) through an electrostatic interaction at physiological pH. The protein non-adsorption capability is comparable to that of PEG-coated surfaces through aminosilanization (unpublished data). A similar strategy for PEGylation, which is not used for single-molecule fluorescence imaging, involves using a poly(L-lysine) grafted with PEG (PLL-g-PEG), a polycationic copolymer that is positively charged at neutral pH. The compound spontaneously adsorbs from aqueous solution onto negatively charged surfaces, resulting in the formation of stable polymeric monolayers and rendering the surfaces protein-resistant to a degree relative to the PEG surface density (Huang et al., 2001; Pasche et al., 2003).

3.2 Lipid bilayer

Artificial lipid membranes deposited on solid supports have proven to be useful for many types of biochemical studies (Chan & Boxer, 2007). The membranes provide a surface environment that is similar to that inside a living cell and can prevent any non-specific interactions of biomolecules on the surface. Lipid bilayers that are spontaneously formed on quartz surfaces have been used for single-molecule fluorescence imaging. The bilayers can be modified through the incorporation of lipids with various functional groups such as biotin or PEG. A mixture of 1,2-dioleoyl-*sn*-glycerophosphocholine dioleoylphosphatidylcholine (DOPC) with a small amount of 1,2-dioleoyl-*sn*-glycero-3-phosphoethanolamine-*N*-[methoxy(polyethylene glycol)-550] (mPEG 550-DOPE) was reported to help minimize non-specific binding of Qdot-tagged proteins to the lipid bilayer (Gorman et al., 2010). For experiments that require tethering DNA that is biotinylated at the end(s), avidin is attached either via non-specific interaction with the glass surface or via interaction with biotin head groups of the lipids present.

4. Platforms

A common feature among direct visualization of single-molecule DNA-binding protein molecules is the need for DNA to be tethered and extended. A pioneering platform

published in 1993 employs dielectrophoresis between aluminium electrodes to extend λDNA (Fig. 6g) (Kabata et al., 1993). λDNA is a bacteriophage DNA that consists of 48,490 base pairs of double-stranded linear DNA with 12-nucleotide single-stranded segments at both 5′ ends (approximately 16.5 μm in total length). The platform can form "DNA belts" and has uncovered RNA polymerase dynamics along DNA, including sliding and jumping. Another pioneering platform published in 1998 employs optical tweezers, which was incorporated into a single-molecule fluorescence microscope, to extend λDNA (Fig. 6d) (Harada et al., 1999), which revealed strain-dependent DNA-binding kinetics of RNA polymerase. At that time, casein, a conventional blocking agent that is found in milk in large quantities, was used to block non-specific protein adsorption.

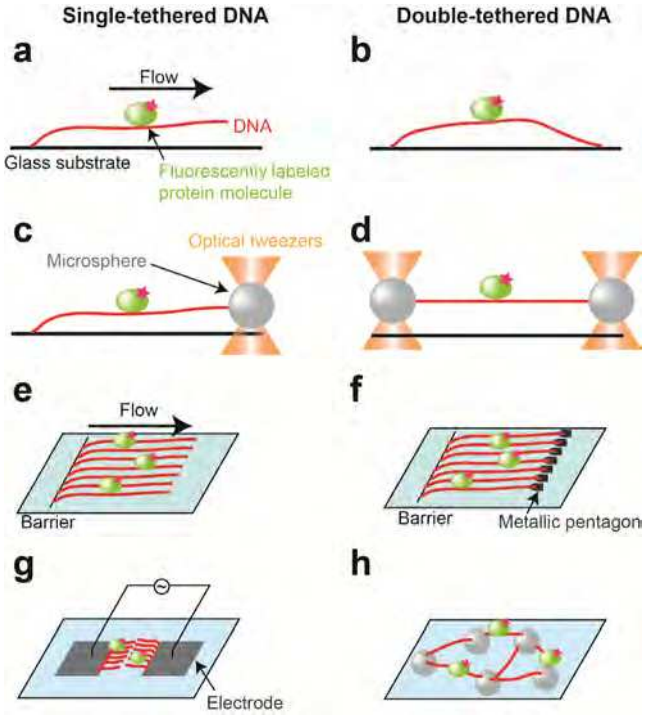

Fig. 6. Platforms used for direct visualization of single-molecule DNA-binding protein molecules along DNA. (a) DNA tethered at one end on a glass surface with buffer flow. (b) DNA tethered at both ends on a glass surface. (c) DNA tethered on a glass surface at one end and with optical tweezers at the other end. (d) DNA tethered with optical tweezers at both ends. (e) DNA curtains. (f) DNA racks. (g) DNA belts. (f) Tightropes.

To minimize non-specific protein adsorption, most of the visualization has been performed on glass surfaces modified by the coating methods discussed in the previous section. Many platforms capable of real-time visualization of single-molecule DNA-binding protein molecules along tethered DNA, most of which are used in combination with total-internal fluorescence microscopy (Funatsu et al., 1995; Tokunaga et al., 1997), have been developed to understand protein dynamics. Among many methods for DNA tethering by non-specific

adsorption, or specific attachments mediated by a non-covalent interaction, the most popular DNA tethering method used for the platforms is tethering biotinylated λDNA on glass surfaces via an avidin-biotin interaction. The two single-stranded segments at both 5′ ends of λDNA, termed the *cos* site, are the sticky ends and can be easily biotinylated via ligation with corresponding the complimentary biotinylated oligos. The biotinylated λDNA can be tethered on glass surfaces at either one or both end(s) via an avidin-biotin interaction. In the following sections, I briefly review some of the modern platforms and present their target DNA protein molecules.

4.1 Platforms with continuous buffer flow

Tethering DNA at one end on the surface via an avidin-biotin interaction is the simplest method for tethering DNA. However, owing to the flexible nature of DNA, tethering alone cannot make the DNA extend sufficiently enough for use in single-molecule visualization with high spatial resolution. To stretch such DNA, some investigators use shear force generated by hydrodynamic flow (Fig. 6a) (Brewer & Bianco, 2008; Graneli et al., 2006; Greene & Mizuuchi, 2002; S. Kim et al., 2007; Lee et al., 2006; van Oijen et al., 2003). In this platform, buffer is continuously input into a flow cell made of sandwiched glass substrates. The glass substrates are coated with PEG (Blainey et al., 2006; Blainey et al., 2009; S. Kim et al., 2007) or a lipid bilayer (Graneli et al., 2006) to reduce non-specific adsorption of protein molecules. With this platform, dynamics of many single-molecule proteins have been uncovered. These include dynamics of single-protein polymers along DNA (Greene & Mizuuchi, 2002; Han & Mizuuchi, 2010; Tan et al., 2007) and one-dimensional diffusion of many DNA-binding protein molecules, for example, a base-excision DNA-repair protein along DNA (Blainey et al., 2006; Etson et al., 2010; Kochaniak et al., 2009; Komazin-Meredith et al., 2008; Tafvizi et al., 2011). A comparison of one-dimensional diffusion constants as a function of protein size with theoretical predictions indicates that DNA-binding proteins undergo rotation-coupled sliding along the DNA helix (Blainey et al., 2009).

4.2 Tethering DNA at multiple points on glass surfaces

As mentioned above, tethering DNA at one end on the surface alone is not sufficient for the single-molecule visualization. Several papers report methods of DNA tethering at many points via non-specific interaction or at both ends (Fig. 6b) on the surface via an avidin-biotin interaction. These include λDNA immobilized on a polystyrene-coated coverslip via a non-specific interaction (Kim & Larson, 2007) or on a lipid bilayer-deposited fused silica slide via an avidin-biotin interaction (Graneli et al., 2006), and T7 bacteriophage DNA immobilized on a silanized coverslip via an avidin-biotin interaction (Bonnet et al., 2008). Using these platforms, one-dimensional diffusion and transcription of single T7 RNA polymerases along DNA (Kim & Larson, 2007) and sliding and jumping of EcoRV restriction enzyme (Bonnet et al., 2008) along DNA were visualized.

4.3 DNA curtains

4.3.1 Single-tethered DNA curtains

To tether many DNA strands on the surface for a high-throughput single-molecule analysis, the Greene group has developed a new platform referred to as ‘‘DNA curtains’’ (Fig. 6e) (Fazio

et al., 2008; Graneli et al., 2006; Visnapuu et al., 2008). This assay allows simultaneous study of up to hundreds of individual DNA strands anchored to a lipid bilayer and aligned with respect to one another within a single field-of-view with TIRFM. The DNA curtains were constructed in the following manner: (i) the surface of a glass slide was first mechanically etched to form lipid-diffusion barriers perpendicular to the direction of buffer flow. (ii) The flow cell was coated with a lipid bilayer by injecting lipid vesicles comprising DOPC, biotinylated lipids, and PEGylated lipids into the sample chamber (discussed in 3.2). (iii) After removing the excess vesicles by a buffer flush, neutravidin was injected into the flow cell. (iv) λDNA that was biotinylated at one end was injected into the flow cell. The PEGylated lipid enhanced protein non-specific adsorption suppression capability on the surface. The barriers formed on the flow cell could not be traversed by the lipids, and thus, buffer flow extended the lipid-tethered DNA in the flow direction and confined the DNA within the evanescent field generated by total-internal reflection. This platform has been used to study a broad range of DNA-binding proteins that function in homologous recombination (Prasad et al., 2006; Prasad et al., 2007) and mismatch repair (Gorman et al., 2007).

4.3.2 Double-tethered DNA curtains

The DNA curtains require buffer flow to extend DNA for single-molecule visualization of protein dynamics along the DNA. The hydrodynamic force exerted by the buffer flow can potentially influence the behavior of protein molecules; this influence is expected to be proportional to the hydrodynamic radius of the protein molecules under observation (Gorman & Greene, 2008; Tafvizi et al., 2008). To circumvent such an issue, the Greene group has developed double-tethered DNA curtains without the need of buffer flow during the visualization (Fig. 6f) (Gorman et al., 2010). The group used electron beam lithography to fabricate diffusion barriers with nanoscale dimensions, which allows for much more precise control over both the location and lateral distribution of the DNA within the curtains. These patterns, which the group termed "DNA racks," comprise linear barriers to lipid diffusion along with arrays of metallic pentagons, which are used for the scaffold of antibodies to anchor DNA at one end. The lipid-tethered DNA is first aligned along the linear barriers; subsequently, the DNA is anchored on the pentagons positioned at a defined distance downstream from the linear barriers. Once aligned and anchored, the "double-tethered" DNA curtains maintain their extended form. This sophisticated platform has been applied to biological systems such as nucleosomes and chromatin remodeling (Fig. 7) (Finkelstein et al., 2010; Gorman et al., 2010).

4.4 DNA tightropes

Another platform that did not require buffer flow was developed for single-molecule visualization of protein dynamics along extended DNA. In this platform, λDNA is suspended between poly (L-lysine)-coated microspheres non-specifically attached on a PEGylated surface to form "DNA tightropes" in a flow cell, allowing the DNA to maintain its extended form during the visualization (Fig. 6h) (Kad et al., 2010). Since DNA is negatively charged at physiological pH, DNA can attach to the positively charged poly (L-lysine) that is coated on the microspheres via an electrostatic interaction. Injection of high concentration of DNA (1.6 nM) forms many DNA tightropes, allowing a high-throughput single-molecule analysis by simultaneous observation of multiple DNA-binding protein

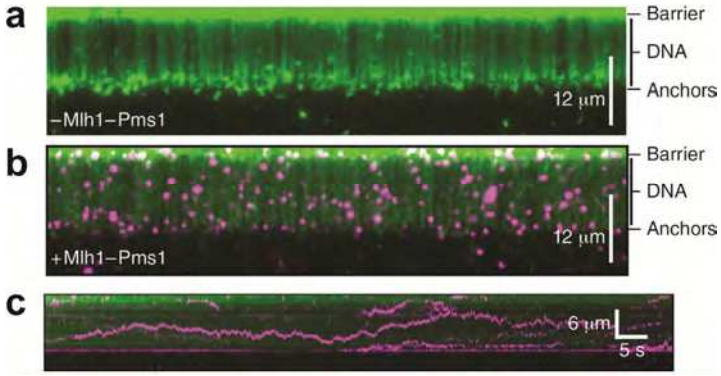

Fig. 7. Nanofabricated racks of DNA for visualizing one-dimensional diffusion of a postreplicative mismatch repair protein complex (Mlh1–Pms1). (a) YOYO1-stained λDNA curtains (green; 48,502 base pairs), (b) YOYO1-stained λDNA curtains with a Qdot-labeled protein complex (magenta), and (c) Kymogram illustrating the motion of the protein complex. (Modified from *Nature Structural & Molecular Biology* (Gorman et al., 2010) , Copyright (2010), with permission from Macmillan Publishers Ltd).

molecules. Since the DNA tightropes formed on the microspheres are off the glass surface, there is no interaction between the DNA and the glass surface, which may not interfere with the interactions with the protein molecules. Furthermore, the no buffer-flow condition enables the detection of various dynamic mechanisms of DNA repair proteins, including not only diffusion along DNA (Dunn et al., 2011) but also jumping from one DNA to another DNA (Fig. 8) (Kad et al., 2010).

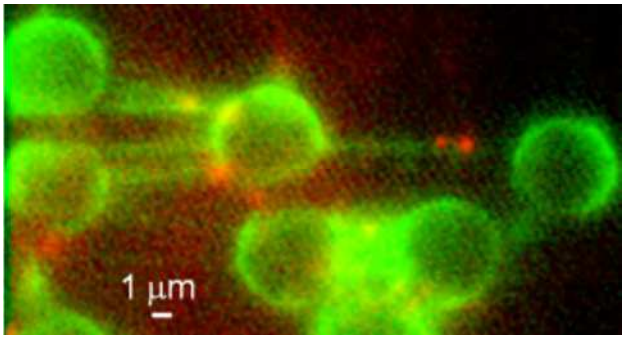

Fig. 8. Fluorescence image of Qdot-labeled single protein molecules (UvrA, red spots) bound to DNA tightropes (green). (Reproduced from (Kad et al., 2010), Copyright (2010), with permission from Elsevier).

4.4.1 Minimization of protein non-specific adsorption on microspheres by PEGylaton

One of the drawbacks of the DNA tightrope platform with poly (L-lysine)-coated microspheres is that many protein molecules are non-specifically adsorbed on the microspheres. Fluorescence from the Qdots that are labeled to the adsorbed protein

molecules interferes with single-molecule fluorescence imaging. Kad et al. circumvented the interference by manually masking the bead portions on screen using an image analysis software before analysis (Kad et al., 2010). Here, I describe another tightrope platform developed to overcome the issue by PEGylation, in which the glass surface as well as microspheres are coated with biotinylated PEG. The excellent resistance of PEG to protein adsorption (discussed in 3.1) efficiently suppresses the non-specific adsorption of Qdot-labeled protein molecules on the microspheres. The biotin of the PEG allows the microspheres to be immobilized on the glass surface and biotinylated DNA to be tethered between the microspheres via an avidin-biotin interaction (Fig. 9). With this improved platform, dynamics of a DNA repair protein is currently being investigated.

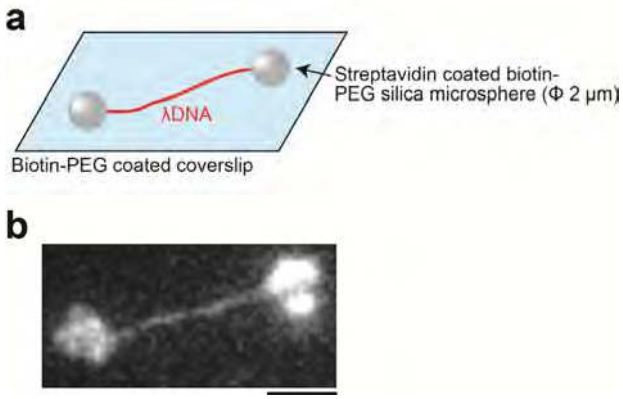

Fig. 9. A tightrope formed between streptavidin coated biotin-PEG silica microspheres immobilized on a biotin-PEG coated coverslip. (a) Schematic drawing of this tightrope platform. (b) Fluorescence image of YOYO1-labeled λDNA tethered between microspheres. Scale bar, 5 μm.

4.5 DNA extended by single-molecule DNA manipulation

Technical advances in combining single-molecule fluorescence visualization with single-molecule manipulation provide deeper insights into DNA–protein interactions. Some groups incorporated optical tweezers into a single-molecule fluorescence set-up (Fig. 6c,d) for studying DNA dynamics or DNA–protein interactions (Amitani et al., 2006; Comstock et al., 2011; Galletto et al., 2006; Harada et al., 1999; Hohng et al., 2007; Lang et al., 2004; van Mameren et al., 2009; Zhou et al., 2011). With such platforms, translocation (Amitani et al., 2006), association and dissociation (Harada et al., 1999; Zhou et al., 2011), filament assembly (Galletto et al., 2006), and disassembly (van Mameren et al., 2009) of protein molecules along DNA were visualized. Some of these studies investigated the effect of DNA tension on DNA–protein interactions. Recently, my colleagues and I have incorporated magnetic tweezers (Allemand et al., 2007), another apparatus for single-molecule DNA manipulation, into the single-molecule fluorescence set-up through collaboration with my research colleagues, which has allowed us to visualize single-molecule DNA helicase interacting with single dsDNA that is tethered by the magnetic tweezers.

5. Outlook

I have provided an overview recent of advances in direct visualization of single-molecule DNA-binding proteins, especially of key techniques used for the visualization. Fluorescence labeling methods as well as modern platforms employing biocompatible surface-coating methods described here have allowed the dynamics of single-molecule DNA-binding proteins to be elucidated. Frequently used fluorophores, dyes and Qdots have allowed visualization to a certain extent. However, the fluorophores have not satisfied all the requirements related to optimum size and photophysical properties, for example, dyes are small but short lived whereas Qdots are bright and resistant to photobleaching, but relatively large in size. Thus, it is highly desirable that new all-round fluorophores be synthesized or extracted from materials. One such promising fluorophore is the nitrogen-vacancy center, a crystal defect in diamonds (Aharonovich et al., 2011). The defect that emits near-infrared fluorescence exhibits neither blinking nor photobleaching, which is distinct from the common fluorophores.

Technical advances in combining single-molecule fluorescence visualization with single-molecule manipulation (discussed in 4.5) will provide deeper insights into DNA–protein interactions. Zero-mode waveguides (Levene et al., 2003), a nano-hole (<100 nm in diameter) array, is another promising microscopy for visualizing DNA–protein interactions. The waveguides attract increasing attention because compared to TIRFM, zero-mode waveguides make it possible to perform single-molecule fluorescence imaging under higher ligand concentration (μM range) conditions due to its extremely small excitation volume. And thus, a few biological processes were visualized at single-molecule resolution by zero-mode waveguides (Miyake et al., 2008; Sameshima et al., 2010; Uemura et al., 2010).

In a recent study (Kad et al., 2010), single-molecule interaction of two different DNA protein molecules along DNA was visualized by labeling them with different fluorophores, although most studies typically focused on the dynamics of single DNA binding-proteins. In the future, simultaneous visualization of different DNA-binding protein molecules may be possible by labeling the molecules with different fluorophores. This will help elucidate fundamental processes of DNA metabolism. In fact, biological processes in DNA metabolism involve various protein molecules as a form of macromolecular complexes. Moreover, the processes can be associated with chromatin for eukaryotes. To approach the protein dynamics in such an environment, a recent study investigated single-molecule interaction between a protein complex and chromatin (Gorman et al., 2010). Future developments in various fields, including platforms, fluorophores, surface coating, and fluorescence labelling, will provide fruitful information on complex DNA–protein interactions that cannot otherwise be explored.

6. Acknowledgments

I would like to thank the Harada group at Kyoto University and the Bensimon & Croquette group at École Normale Supérieure for supporting my research. The presented work performed in the groups was partly funded by JSPS and JST.

7. References

Aharonovich, I., Greentree, A. D. & Prawer, S. (2011). Diamond photonics. *Nature Photonics,* 5(7), 397-405.

Aitken, C. E., Marshall, R. A. & Puglisi, J. D. (2008). An oxygen scavenging system for improvement of dye stability in single-molecule fluorescence experiments. *Biophysical Journal,* 94(5), 1826-1835.

Allemand, J.-F., Bensimon, D., Charvin, G., Croquette, V., Lia, G., Lionnet, T., Neuman, K. C., Saleh, O. A. & Yokota, H. (2007). Studies of DNA-Protein Interactions at the single molecule level with magnetic tweezers. *Lecture Notes on Physics,* 711, 123-140.

Amitani, I., Baskin, R. J. & Kowalczykowski, S. C. (2006). Visualization of Rad54, a chromatin remodeling protein, translocating on single DNA molecules. *Molecular Cell,* 23(1), 143-148.

Anderson, A. S., Dattelbaum, A. M., Montano, G. A., Price, D. N., Schmidt, J. G., Martinez, J. S., Grace, W. K., Grace, K. M. & Swanson, B. I. (2008). Functional PEG-modified thin films for biological detection. *Langmuir,* 24(5), 2240-2247.

Blainey, P. C., van Oijen, A. M., Banerjee, A., Verdine, G. L. & Xie, X. S. (2006). A base-excision DNA-repair protein finds intrahelical lesion bases by fast sliding in contact with DNA. *Proceedings of the National Academy of Sciences of the United States of America,* 103(15), 5752-5757.

Blainey, P. C., Luo, G., Kou, S. C., Mangel, W. F., Verdine, G. L., Bagchi, B. & Xie, X. S. (2009). Nonspecifically bound proteins spin while diffusing along DNA. *Nature Structural & Molecular Biology,* 16(12), 1224-1229.

Bonnet, I., Biebricher, A., Porte, P. L., Loverdo, C., Benichou, O., Voituriez, R., Escude, C., Wende, W., Pingoud, A. & Desbiolles, P. (2008). Sliding and jumping of single EcoRV restriction enzymes on non-cognate DNA. *Nucleic Acids Research,* 36(12), 4118-4127.

Branch, D. W., Wheeler, B. C., Brewer, G. J. & Leckband, D. E. (2001). Long-term stability of grafted polyethylene glycol surfaces for use with microstamped substrates in neuronal cell culture. *Biomaterials,* 22(10), 1035-1047.

Brewer, L. R. & Bianco, P. R. (2008). Laminar flow cells for single-molecule studies of DNA-protein interactions. *Nature Methods,* 5(6), 517-525.

Chan, Y. H. & Boxer, S. G. (2007). Model membrane systems and their applications. *Current Opinion in Chemical Biology,* 11(6), 581-587.

Comstock, M. J., Ha, T. & Chemla, Y. R. (2011). Ultrahigh-resolution optical trap with single-fluorophore sensitivity. *Nature Methods,* 8(4), 335-340.

Cuvelier, D., Rossier, O., Bassereau, P. & Nassoy, P. (2003). Micropatterned "adherent/repellent" glass surfaces for studying the spreading kinetics of individual red blood cells onto protein-decorated substrates. *European Biophysics Journal,* 32(4), 342-354.

Dave, R., Terry, D. S., Munro, J. B. & Blanchard, S. C. (2009). Mitigating unwanted photophysical processes for improved single-molecule fluorescence imaging. *Biophysical Journal,* 96(6), 2371-2381.

Dunn, A. R., Kad, N. M., Nelson, S. R., Warshaw, D. M. & Wallace, S. S. (2011). Single Qdot-labeled glycosylase molecules use a wedge amino acid to probe for lesions while scanning along DNA. *Nucleic Acids Research,* 39(17), 7487-7498.

Etson, C. M., Hamdan, S. M., Richardson, C. C. & van Oijen, A. M. (2010). Thioredoxin suppresses microscopic hopping of T7 DNA polymerase on duplex DNA. *Proceedings of the National Academy of Sciences of the United States of America,* 107(5), 1900-1905.

Fazio, T., Visnapuu, M. L., Wind, S. & Greene, E. C. (2008). DNA curtains and nanoscale curtain rods: high-throughput tools for single molecule imaging. *Langmuir,* 24(18), 10524-10531.

Fernández-Suárez, M. & Ting, A. Y. (2008). Fluorescent probes for super-resolution imaging in living cells. *Nature Reviews Molecular Cell Biology,* 9(12), 929-943.

Finkelstein, I. J., Visnapuu, M. L. & Greene, E. C. (2010). Single-molecule imaging reveals mechanisms of protein disruption by a DNA translocase. *Nature,* 468(7326), 983-987.

Funatsu, T., Harada, Y., Tokunaga, M., Saito, K. & Yanagida, T. (1995). Imaging of single fluorescent molecules and individual ATP turnovers by single myosin molecules in aqueous solution. *Nature,* 374(6522), 555-559.

Galletto, R., Amitani, I., Baskin, R. J. & Kowalczykowski, S. C. (2006). Direct observation of individual RecA filaments assembling on single DNA molecules. *Nature,* 443(7113), 875-878.

Gorman, J., Chowdhury, A., Surtees, J. A., Shimada, J., Reichman, D. R., Alani, E. & Greene, E. C. (2007). Dynamic basis for one-dimensional DNA scanning by the mismatch repair complex Msh2-Msh6. *Molecular Cell,* 28(3), 359-370.

Gorman, J. & Greene, E. C. (2008). Visualizing one-dimensional diffusion of proteins along DNA. *Nature Structural & Molecular Biology,* 15(8), 768-774.

Gorman, J., Fazio, T., Wang, F., Wind, S. & Greene, E. C. (2010). Nanofabricated racks of aligned and anchored DNA substrates for single-molecule imaging. *Langmuir,* 26(2), 1372-1379.

Gorman, J., Plys, A. J., Visnapuu, M. L., Alani, E. & Greene, E. C. (2010). Visualizing one-dimensional diffusion of eukaryotic DNA repair factors along a chromatin lattice. *Nature Structural & Molecular Biology,* 17(8), 932-938.

Graneli, A., Yeykal, C. C., Prasad, T. K. & Greene, E. C. (2006). Organized arrays of individual DNA molecules tethered to supported lipid bilayers. *Langmuir,* 22(1), 292-299.

Greene, E. C. & Mizuuchi, K. (2002). Direct observation of single MuB polymers: evidence for a DNA-dependent conformational change for generating an active target complex. *Molecular Cell,* 9(5), 1079-1089.

Ha, T., Rasnik, I., Cheng, W., Babcock, H. P., Gauss, G. H., Lohman, T. M. & Chu, S. (2002). Initiation and re-initiation of DNA unwinding by the *Escherichia coli* Rep helicase. *Nature,* 419(6907), 638-641.

Ha, T. (2004). Structural dynamics and processing of nucleic acids revealed by single-molecule spectroscopy. *Biochemistry,* 43(14), 4055-4063.

Han, S., Kim, C. & Kwon, D. (1997). Thermal/oxidative degradation and stabilization of polyethylene glycol. *Polymer,* 38, 317-323.

Han, Y. W. & Mizuuchi, K. (2010). Phage Mu transposition immunity: protein pattern formation along DNA by a diffusion-ratchet mechanism. *Molecular Cell,* 39(1), 48-58.

Harada, Y., Sakurada, K., Aoki, T., Thomas, D. D. & Yanagida, T. (1990). Mechanochemical coupling in actomyosin energy transduction studied by *in vitro* movement assay. *Journal of Molecular Biology,* 216(1), 49-68.

Harada, Y., Funatsu, T., Murakami, K., Nonoyama, Y., Ishihama, A. & Yanagida, T. (1999). Single-molecule imaging of RNA polymerase-DNA interactions in real time. *Biophysical Journal,* 76(2), 709-715.

Harris, J. M. (1992). *Poly(Ethylene Glycol) Chemistry (Ethylene Glycol Chemistry : Biotechnical and Biomedical Applications)*. New York: Plenum Press.

Hermanson, G. T. (2008). *Bioconjugate Techniques (2nd Edition)*: Academic Press.

Heyes, C. D., Kobitski, A. Y., Amirgoulova, E. V. & Nienhaus, G. U. (2004). Biocompatible surfaces for specific tethering of individual protein molecules. *Journal of Physical Chemistry B,* 108(35), 13387-13394.

Hilario, J. & Kowalczykowski, S. C. (2010). Visualizing protein-DNA interactions at the single-molecule level. *Current Opinion in Chemical Biology,* 14(1), 15-22.

Hohng, S., Zhou, R., Nahas, M. K., Yu, J., Schulten, K., Lilley, D. M. & Ha, T. (2007). Fluorescence-force spectroscopy maps two-dimensional reaction landscape of the holliday junction. *Science,* 318(5848), 279-283.

Huang, N.-P., Michel, R., Voros, J., Textor, M., Hofer, R., Rossi, A., Elbert, D. L., Hubbell, J. A. & Spencer, N. D. (2001). Poly(L-lysine)-g-poly(ethylene glycol) layers on metal oxide surfaces: surface-analytical characterization and resistance to serum and fibrinogen adsorption. *Langmuir,* 17(2), 489-498.

Iler, R. K. (1979). *The Chemistry of Silica*. New York: Wiley-Interscience.

Ito, Y., Hasuda, H., Sakuragi, M. & Tsuzuki, S. (2007). Surface modification of plastic, glass and titanium by photoimmobilization of polyethylene glycol for antibiofouling. *Acta Biomaterialia,* 3(6), 1024-1032.

Joo, C., McKinney, S. A., Nakamura, M., Rasnik, I., Myong, S. & Ha, T. (2006). Real-time observation of RecA filament dynamics with single monomer resolution. *Cell,* 126(3), 515-527.

Kabata, H., Kurosawa, O., Arai, I., Washizu, M., Margarson, S. A., Glass, R. E. & Shimamoto, N. (1993). Visualization of single molecules of RNA polymerase sliding along DNA. *Science,* 262(5139), 1561-1563.

Kad, N. M., Wang, H., Kennedy, G. G., Warshaw, D. M. & Van Houten, B. (2010). Collaborative dynamic DNA scanning by nucleotide excision repair proteins investigated by single-molecule imaging of quantum-dot-labeled proteins. *Molecular Cell,* 37(5), 702-713.

Kim, J. H. & Larson, R. G. (2007). Single-molecule analysis of 1D diffusion and transcription elongation of T7 RNA polymerase along individual stretched DNA molecules. *Nucleic Acids Research,* 35(11), 3848-3858.

Kim, S., Blainey, P. C., Schroeder, C. M. & Xie, X. S. (2007). Multiplexed single-molecule assay for enzymatic activity on flow-stretched DNA. *Nature Methods,* 4(5), 397-399.

Kochaniak, A. B., Habuchi, S., Loparo, J. J., Chang, D. J., Cimprich, K. A., Walter, J. C. & van Oijen, A. M. (2009). Proliferating cell nuclear antigen uses two distinct modes to move along DNA. *Journal of Biological Chemistry,* 284(26), 17700-17710.

Komazin-Meredith, G., Mirchev, R., Golan, D. E., van Oijen, A. M. & Coen, D. M. (2008). Hopping of a processivity factor on DNA revealed by single-molecule assays of diffusion. *Proceedings of the National Academy of Sciences of the United States of America,* 105(31), 10721-10726.

Lang, M. J., Fordyce, P. M., Engh, A. M., Neuman, K. C. & Block, S. M. (2004). Simultaneous, coincident optical trapping and single-molecule fluorescence. *Nature Methods,* 1(2), 133-139.

Lee, J. B., Hite, R. K., Hamdan, S. M., Xie, X. S., Richardson, C. C. & van Oijen, A. M. (2006). DNA primase acts as a molecular brake in DNA replication. *Nature,* 439(7076), 621-624.

Levene, M. J., Korlach, J., Turner, S. W., Foquet, M., Craighead, H. G. & Webb, W. W. (2003). Zero-mode waveguides for single-molecule analysis at high concentrations. *Science,* 299(5607), 682-686.

Lohman, T. M., Tomko, E. J. & Wu, C. G. (2008). Non-hexameric DNA helicases and translocases: mechanisms and regulation. *Nature Reviews Molecular Cell Biology,* 9(5), 391-401.

Malmstena, M., Emoto, K. & Alstine, J. M. V. (1998). Effect of chain density on inhibition of protein adsorption by poly(ethylene glycol) Based Coatings. *Journal of Colloid Interface Science,* 202(2), 507-517.

Maluf, N. K., Fischer, C. J. & Lohman, T. M. (2003). A dimer of *Escherichia coli* UvrD is the active form of the helicase in vitro. *Journal of Molecular Biology,* 325(5), 913-935.

McNamee, C. E., Yamamoto, S. & Higashitani, K. (2007). Preparation and characterization of pure and mixed monolayers of poly(ethylene glycol) brushes chemically adsorbed to silica surfaces. *Langmuir,* 23(8), 4389-4399.

Michalet, X., Pinaud, F. F., Bentolila, L. A., Tsay, J. M., Doose, S., Li, J. J., Sundaresan, G., Wu, A. M., Gambhir, S. S. & Weiss, S. (2005). Quantum dots for live cells, *in vivo* imaging, and diagnostics. *Science,* 307(5709), 538-544.

Miyake, T., Tanii, T., Sonobe, H., Akahori, R., Shimamoto, N., Ueno, T., Funatsu, T. & Ohdomari, I. (2008). Real-time imaging of single-molecule fluorescence with a zero-mode waveguide for the analysis of protein-protein interaction. *Analytical Chemistry,* 80(15), 6018-6022.

Moerner, W. E. (2007). Single-molecule Chemistry and Biology Special Feature: New directions in single-molecule imaging and analysis. *Proceedings of the National Academy of Sciences of the United States of America,* 104(31), 12596-12602.

Pasche, S., Paul, S. M. D., Vörös, J., Spencer, N. D. & Textor, M. (2003). Poly(L-lysine)-graft-poly(ethyleneglycol) assembled monolayers on niobium oxide surfaces: a quantitative study of the influence of polymer interfacial architecture on resistance to protein adsorption by ToF-SIMS and *in situ* OWLS. *Langmuir,* 19, 9216-9235.

Prasad, T. K., Yeykal, C. C. & Greene, E. C. (2006). Visualizing the assembly of human Rad51 filaments on double-stranded DNA. *Journal of Molecular Biology,* 363(3), 713-728.

Prasad, T. K., Robertson, R. B., Visnapuu, M. L., Chi, P., Sung, P. & Greene, E. C. (2007). A DNA-translocating Snf2 molecular motor: *Saccharomyces cerevisiae* Rdh54 displays processive translocation and extrudes DNA loops. *Journal of Molecular Biology,* 369(4), 940-953.

Prime, K. L. & Whitesides, G. M. (1991). Self-assembled organic monolayers: model systems for studying adsorption of proteins at surfaces. *Science,* 252(5010), 1164-1167.

Rasnik, I., McKinney, S. A. & Ha, T. (2006). Nonblinking and long-lasting single-molecule fluorescence imaging. *Nature Methods,* 3(11), 891-893.

Sameshima, T., Iizuka, R., Ueno, T., Wada, J., Aoki, M., Shimamoto, N., Ohdomari, I., Tanii, T. & Funatsu, T. (2010). Single-molecule study on the decay process of the football-shaped GroEL-GroES complex using zero-mode waveguides. *Journal of Biological Chemistry,* 285(30), 23159-23164.

Sharma, S., Johnson, R. W. & Desai, T. A. (2004). Evaluation of the stability of nonfouling ultrathin poly(ethylene glycol) films for silicon-based microdevices. *Langmuir,* 20(2), 348-356.

Tafvizi, A., Huang, F., Leith, J. S., Fersht, A. R., Mirny, L. A. & van Oijen, A. M. (2008). Tumor suppressor p53 slides on DNA with low friction and high stability. *Biophysical Journal,* 95(1), L01-03.

Tafvizi, A., Huang, F., Fersht, A. R., Mirny, L. A. & van Oijen, A. M. (2011). A single-molecule characterization of p53 search on DNA. *Proceedings of the National Academy of Sciences of the United States of America,* 108(2), 563-568.

Tan, X., Mizuuchi, M. & Mizuuchi, K. (2007). DNA transposition target immunity and the determinants of the MuB distribution patterns on DNA. *Proceedings of the National Academy of Sciences of the United States of America,* 104(35), 13925-13929.

Tokunaga, M., Kitamura, K., Saito, K., Iwane, A. H. & Yanagida, T. (1997). Single molecule imaging of fluorophores and enzymatic reactions achieved by objective-type total internal reflection fluorescence microscopy. *Biochemical and Biophysical Research Communications,* 235(1), 47-53.

Tokunaga, M., Imamoto, N. & Sakata-Sogawa, K. (2008). Highly inclined thin illumination enables clear single-molecule imaging in cells. *Nature Methods,* 5(2), 159-161.

Uemura, S., Aitken, C. E., Korlach, J., Flusberg, B. A., Turner, S. W. & Puglisi, J. D. (2010). Real-time tRNA transit on single translating ribosomes at codon resolution. *Nature,* 464(7291), 1012-1017.

van Mameren, J., Modesti, M., Kanaar, R., Wyman, C., Peterman, E. J. & Wuite, G. J. (2009). Counting RAD51 proteins disassembling from nucleoprotein filaments under tension. *Nature,* 457(7230), 745-748.

van Oijen, A. M., Blainey, P. C., Crampton, D. J., Richardson, C. C., Ellenberger, T. & Xie, X. S. (2003). Single-molecule kinetics of lambda exonuclease reveal base dependence and dynamic disorder. *Science,* 301(5637), 1235-1238.

Visnapuu, M. L., Duzdevich, D. & Greene, E. C. (2008). The importance of surfaces in single-molecule bioscience. *Molecular Biosystems,* 4(5), 394-403.

Wang, X., Ren, X., Kahen, K., Hahn, M. A., Rajeswaran, M., Maccagnano-Zacher, S., Silcox, J., Cragg, G. E., Efros, A. L. & Krauss, T. D. (2009). Non-blinking semiconductor nanocrystals. *Nature,* 459(7247), 686-689.

Yang, Z., Galloway, J. A. & Yu, H. (1999). Protein interactions with poly(ethylene glycol) self-assembled monolayers on glass substrates: diffusion and adsorption *Langmuir,* 15(24), 8405-8411.

Yokota, H., Han, Y. W., Allemand, J.-F., Xi, X. G., Bensimon, D., Croquette, V. & Harada, Y. (2009). Single-molecule visualization of binding modes of helicase to DNA on PEGylated surfaces. *Chemistry Letters,* 38, 308-309.

Zhou, R., Kozlov, A. G., Roy, R., Zhang, J., Korolev, S., Lohman, T. M. & Ha, T. (2011). SSB functions as a sliding platform that migrates on DNA via reptation. *Cell,* 146(2), 222-232.

Zlatanova, J. & van Holde, K. (2006). Single-molecule biology: what is it and how does it work? *Molecular Cell,* 24(3), 317-329.

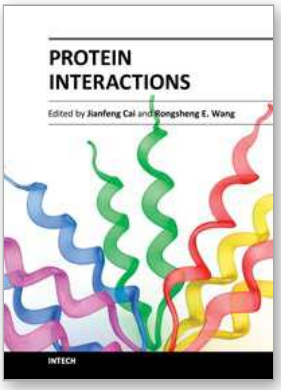

Protein Interactions

Edited by Dr. Jianfeng Cai

ISBN 978-953-51-0244-1
Hard cover, 464 pages
Publisher InTech
Published online 16, March, 2012
Published in print edition March, 2012

Protein interactions, which include interactions between proteins and other biomolecules, are essential to all aspects of biological processes, such as cell growth, differentiation, and apoptosis. Therefore, investigation and modulation of protein interactions are of significance as it not only reveals the mechanism governing cellular activity, but also leads to potential agents for the treatment of various diseases. The objective of this book is to highlight some of the latest approaches in the study of protein interactions, including modulation of protein interactions, development of analytical techniques, etc. Collectively they demonstrate the importance and the possibility for the further investigation and modulation of protein interactions as technology is evolving.

InTech Europe
University Campus STeP Ri
Slavka Krautzeka 83/A
51000 Rijeka, Croatia
Phone: +385 (51) 770 447
Fax: +385 (51) 686 166
www.intechopen.com

InTech China
Unit 405, Office Block, Hotel Equatorial Shanghai
No.65, Yan An Road (West), Shanghai, 200040, China
中国上海市延安西路65号上海国际贵都大饭店办公楼405单元
Phone: +86-21-62489820
Fax: +86-21-62489821